

Substituent dependent layer topologies in copper isophthalate coordination polymers containing long-spanning dipyridylamide ligands



Renee K. Randolph, Robert L. LaDuca*

Lyman Briggs College and Department of Chemistry, Michigan State University, East Lansing, MI, 48825, USA

ARTICLE INFO

Article history:

Received 15 November 2016

Received in revised form

14 January 2017

Accepted 18 January 2017

Available online 19 January 2017

Keywords:

Crystal structure

Coordination polymer

Copper

Layer

Interpenetration

Dipyridylamide

ABSTRACT

Hydrothermal reaction of copper nitrate, a 5-position substituted isophthalic acid, and the long-spanning dipyridylamide ligand 1,6-hexanediaminebis(nicotinamide) (hbn) resulted in two new coordination polymers whose layer topologies and interpenetration mechanisms depend critically on the nature of the substituent. The new phases were structurally characterized by single crystal X-ray diffraction. $\{[\text{Cu}(\text{meoip})(\text{hbn})] \cdot \text{H}_2\text{O}\}_n$ (**1**, meoip = 5-methoxyisophthalate) exhibits $[\text{Cu}(\text{meoip})]_n$ chain motifs with embedded $\{\text{Cu}_2(\text{OCO})_2\}$ dinuclear units, pillared by pairs of hbn ligands into a decorated (4,4) grid topology. $\{[\text{Cu}_3(\text{sip})_2(\text{hbn})_3(\text{H}_2\text{O})_4] \cdot 11.5\text{H}_2\text{O}\}_n$ (**2**, sip = 5-sulfoisophthalate) displays neutral $[\text{Cu}_3(\text{sip})_2(\text{H}_2\text{O})_4]$ fragments connected by hbn ligands into 3,4-connected layer motifs with a $\{4.6^2\}_2\{4^26^28^2\}$ topology, derived from the standard (4,4) grid with regular removal of some pillars. The layer motifs in **2** engage in $2\text{D} + 2\text{D} \rightarrow 3\text{D}$ parallel interpenetration, with entrained co-crystallized water molecule tapes. Thermal decomposition behavior of the new phases is also discussed.

© 2017 Elsevier B.V. All rights reserved.

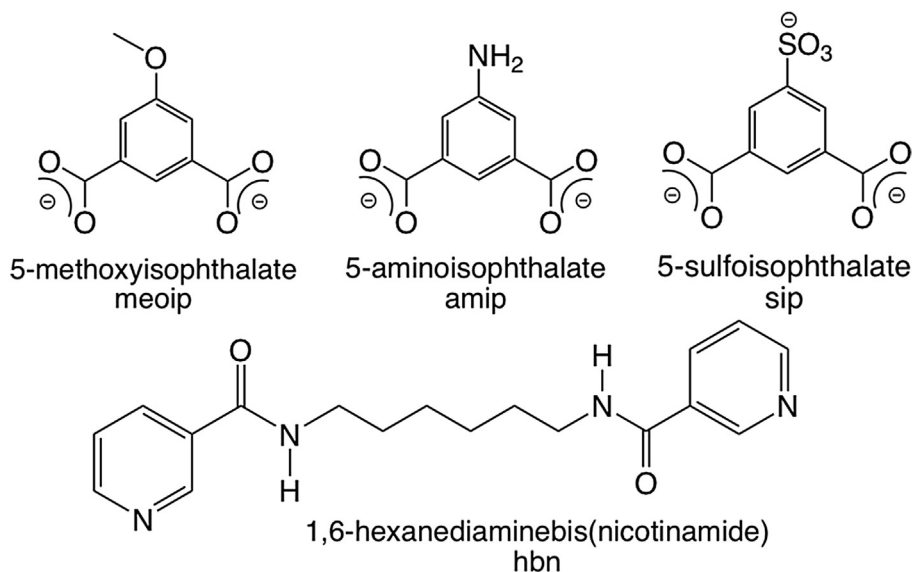
1. Introduction

Exploratory research into the synthesis and property characterization of divalent metal coordination polymers has remained active for over two decades. This genre of materials has shown multifunctional properties such as gas storage [1], selective molecular adsorbing [2], drug-delivery [3], and heterogeneous catalysis [4]. The aesthetic appeal of their underlying molecular structures and topologies has also spurred continued study [5], in addition to the general infrequency of *a priori* structure design [6]. Most reported crystalline coordination polymer solids are based on aromatic dicarboxylate ligands such as isophthalate (ip) [7] or terephthalate [8]. Specific coordination environment preferences at the divalent metal atom, variable carboxylate binding modes, and the inclusion of dipyridyl-type coligands act synergistically during self-assembly to influence the final dimensionality and topology of the final material [9]. One possible means of altering the structural features of an isophthalate-based coordination polymer is to employ derivatives with non-ligating or potentially ligating substituents in the 5-position of the aromatic ring. Yang and co-

workers prepared a series of substituted isophthalate zinc coordination polymers with pyridine capping ligands [10]; sterically bulkier substituents appeared to result in lower coordination polymer dimensionality. Our group observed a similar trend in some substituted isophthalate zinc coordination polymers with the longer-spanning coligand bis(4-pyridylmethyl)piperazine (bpmp) [11,12]. $[\text{Zn}(\text{ip})(\text{bpmp})]_n$ showed a system of five-fold interpenetrated diamondoid nets [11], while $\{[\text{Zn}(\text{meoip})(\text{bpmp})] \cdot 8\text{H}_2\text{O}\}_n$ (meoip = 5-methoxyisophthalate, Scheme 1) adopted an undulating (4,4) grid topology [12]. Inclusion of a ligating sulfonate moiety in the 5-position resulted in $\{[\text{Zn}(\text{sip})(\text{Hbpmp})] \cdot 4\text{H}_2\text{O}\}_n$ (sip = 5-sulfoisophthalate, Scheme 1) which displayed a three-fold interpenetrated binodal lattice with $(4^26)(4^26^58^3)$ topology. Therefore no reduction in dimensionality with respect to the unsubstituted isophthalate derivative was observed in this case, although there was a decrease in interpenetration level. A fascinating self-penetrated structure with a 3,5-connected $(6^3)(6^78^3)$ topology was observed in $\{[\text{Co}(\text{amip})(4\text{-bpmp})] \cdot 3\text{H}_2\text{O}\}_n$ (amip = 5-aminoisophthalate, Scheme 1) [13], showing the versatility of the amip ligand to serve as an exotridentate donor ligand using both of its carboxylate termini as well as its amine group. $\{[\text{Co}(\text{nip})(3\text{-pina})]_n$ (nip = 5-nitroisophthalate, 3-pina = 3-pyridylisonicotinamide) and $\{[\text{Co}(\text{meoip})(3\text{-pina})]_n$ both manifest

* Corresponding author.

E-mail address: laduca@msu.edu (R.L. LaDuca).



Scheme 1. Ligands discussed in this study.

a non-interpenetrated dimer-based 3-D **pcu** network, showing an invariance to the nature of the substituent in the 5-position of the isophthalate ring [14]. Utilizing more flexible dipyridyl coligands has resulted in some intriguing *pseudo*-rotaxane topologies, for instance in $[\text{Co}_2(\text{mip})_2(\text{dpp})_2(\text{H}_2\text{O})]_n$ (mip = 5-methylisophthalate, dpp = 1,3-di(4-pyridyl)propane) [15]. We thus attempted to prepare a series of divalent copper coordination polymers containing 5-substituted isophthalate ligands and the even longer spanning and more flexible dipyridylamide coligand 1,6-hexanediaminebis(nicotinamide) (hbn). This ligand has infrequently been employed in coordination polymer chemistry outside of some work by Wang and colleagues, who reported the synthesis of the 3,4-connected layered phase $\{[\text{Cu}(\text{amip})(\text{hbn})(\text{H}_2\text{O})] \cdot 2\text{H}_2\text{O}\}_n$ in 2013 [16], along with a series of cobalt/hbn coordination polymers with substituted isophthalate ligands [17]. In this contribution we present the single-crystal structures, divergent topological features, and thermal properties of two new layered copper coordination polymers with hbn and substituted isophthalate ligands: $\{[\text{Cu}(\text{meoip})(\text{hbn})] \cdot \text{H}_2\text{O}\}_n$ (**1**) and $\{[\text{Cu}_3(\text{sip})_2(\text{hbn})_3(\text{H}_2\text{O})_4] \cdot 11.5\text{H}_2\text{O}\}_n$ (**2**).

2. Experimental section

2.1. General considerations

Copper nitrate hydrate and 5-methoxyisophthalic acid were commercially obtained from Sigma Aldrich. Sodium 5-sulfoisophthalate was purchased from TCI America. 1,6-hexanediaminebis(nicotinamide) (hbn) was prepared by condensation of 1,6-hexanediamine and two molar equivalents of nicotinoyl chloride hydrochloride in dry pyridine. The reaction mixture was quenched with water, and then the product was isolated via CH_2Cl_2 extraction and removal of solvent *in vacuo* [18]. Water was deionized above 3M Ω -cm in-house. IR spectra were recorded on powdered samples using a Perkin Elmer Spectrum One DRIFT instrument. Thermogravimetric analysis was performed on a TA Instruments Q-50 Thermogravimetric Analyzer with a heating rate of 10 °C/min up to 600 °C. Elemental Analysis was carried out using a Perkin Elmer 2400 Series II CHNS/O Analyzer.

2.2. Preparation of $\{[\text{Cu}(\text{meoip})(\text{hbn})] \cdot \text{H}_2\text{O}\}_n$ (**1**)

$\text{Cu}(\text{NO}_3)_2 \cdot 2.5\text{H}_2\text{O}$ (65 mg, 0.28 mmol), 5-methoxyisophthalic acid (55 mg, 0.28 mmol), and hbn (91 mg, 0.28 mmol) were mixed with 0.55 mL of 1.0 M NaOH solution and 10 mL of distilled H_2O in a 23 mL Teflon-lined acid digestion bomb. The bomb was sealed and heated in an oven at 120 °C for 22 h, and then was cooled slowly to 25 °C. Blue crystals of **1** (115 mg, 68% yield based on Cu) were isolated after washing with distilled water, ethanol, and acetone and drying in air. *Anal. Calc.* for $\text{C}_{27}\text{H}_{30}\text{CuN}_4\text{O}_8$ **1**: C, 53.86; H, 5.02; N, 9.31% Found: C, 53.41; H, 4.98; N, 9.22%. IR (cm^{-1}): 3334 (w), 3100 (w), 1664 (m), 1648 (m), 1618 (m), 1589 (s), 1573 (s), 1541 (m), 1450 (m), 1417 (m), 1396 (s), 1335 (s), 1193 (m), 1129 (m), 1102 (m), 1055 (m), 919 (m), 881 (m), 835 (m), 788 (m), 779 (s), 724 (s), 698 (s), 656 (s).

2.3. Preparation of $\{[\text{Cu}_3(\text{sip})_2(\text{hbn})_3(\text{H}_2\text{O})_4] \cdot 11.5\text{H}_2\text{O}\}_n$ (**2**)

$\text{Cu}(\text{NO}_3)_2 \cdot 2.5\text{H}_2\text{O}$ (65 mg, 0.28 mmol), sodium 5-sulfoisophthalate (75 mg, 0.28 mmol), and hbn (91 mg, 0.28 mmol) were mixed with 0.55 mL of 1.0 M NaOH solution and 10 mL of distilled H_2O in a 23 mL Teflon-lined acid digestion bomb. The bomb was sealed and heated in an oven at 120 °C for 22 h, and then was cooled slowly to 25 °C. Blue crystals of **2** (128 mg, 71% yield based on Cu) were isolated after washing with distilled water, ethanol, and acetone and drying in air. *Anal. Calc.* for $\text{C}_{70}\text{H}_{103}\text{Cu}_3\text{N}_{12}\text{O}_{35}\text{S}_2$ **2**: C, 43.62; H, 5.39; N, 8.72% Found: C, 43.43; H, 5.09; N, 8.58%. IR (cm^{-1}): 3286 (w), 2923 (w), 1658 (m), 1604 (m), 1541 (s), 1488 (m), 1433 (m), 1358 (s), 1235 (m), 1204 (m), 1165 (m), 1103 (m), 1060 (m), 1034 (s), 997 (m), 837 (m), 774 (m), 738 (s), 696 (s), 681 (s), 658 (s).

3. X-ray crystallography

Diffraction data for **1** and **2** were collected on a Bruker-AXS SMART-CCD X-ray diffractometer using graphite-monochromated Mo-K α radiation ($\lambda = 0.71073$ Å) at 173 K. The data were processed via SAINT [19], and corrected for both Lorentz and polarization effects and absorption effects using SADABS [20]. The structures were solved using direct methods with SHELXTL [21]

Table 1
Crystal and structure refinement data for **1–2**.

Data	1	2
Empirical formula	C ₂₇ H ₃₀ CuN ₄ O ₈	C ₇₀ H ₁₀₃ Cu ₃ N ₁₂ O ₃₅ S ₂
Formula weight	602.09	1935.38
Crystal system	triclinic	triclinic
Space group	$P\bar{1}$	$P\bar{1}$
<i>a</i> (Å)	10.0276 (10)	11.3632 (8)
<i>b</i> (Å)	10.1545 (10)	12.6658 (9)
<i>c</i> (Å)	14.0842 (14)	15.9665 (12)
α (°)	90.3293 (13)	97.7157 (8)
β (°)	90.6441 (12)	90.9055 (8)
γ (°)	109.5318 (11)	108.7680 (8)
<i>V</i> (Å ³)	1351.4 (2)	2151.8 (3)
<i>Z</i>	2	1
<i>D</i> (g cm ⁻³)	1.480	1.494
μ (mm ⁻¹)	0.865	0.877
Min./max. transmission	0.9030	0.9471
<i>hkl</i> ranges	$-12 \leq h \leq 12,$ $-12 \leq k \leq 12,$ $-16 \leq l \leq 16$	$-13 \leq h \leq 13,$ $-15 \leq k \leq 15,$ $-19 \leq l \leq 19,$
Total reflections	21818	35739
Unique reflections	4937	7901
<i>R</i> (int)	0.0386	0.0352
Parameters	327	582
<i>R</i> ₁ (all data)	0.0627	0.0547
<i>R</i> ₁ (<i>I</i> > 2 σ (<i>I</i>))	0.0539	0.0456
<i>wR</i> ₂ (all data)	0.1466	0.1305
<i>wR</i> ₂ (<i>I</i> > 2 σ (<i>I</i>))	0.1411	0.1222
Max/min residual (e ⁻ /Å ³)	0.981/−1.028	1.179/−0.521
G.O.F.	1.057	1.056

within the OLEX2 crystallographic software suite [22]. All non-hydrogen atoms were refined anisotropically. Hydrogen atoms were placed in calculated positions and refined isotropically with a riding model. Crystallographic details for **1** and **2** are given in Table 1.

4. Results and discussion

4.1. Synthesis and spectra

A crystalline sample of **1** was produced by the hydrothermal reaction of copper nitrate, the 5-methoxyisophthalic acid, and hbn in the presence of aqueous base. Compound **2** was prepared by hydrothermal reaction of copper nitrate, sodium 5-sulfoisophthalate, and hbn. The infrared spectra of **1** and **2** were consistent with their structural components as determined by single-crystal X-ray diffraction. Intense, broad asymmetric and symmetric C–O stretching bands within the carboxylate ligands were observed at 1573 and 1335 cm⁻¹ for **1**, and at 1541 and 1358 cm⁻¹ for **2**. Moderate intensity bands in the range of ~1600 cm⁻¹ to ~1300 cm⁻¹ are attributed to the stretching modes of the pyridyl rings of the hbn ligands [23]. Features corresponding to C–H bending and ring puckering within the pyridyl moieties exist in the region between ~900 and ~650 cm⁻¹. Broad, weak spectral bands in the vicinity of ~3000–3400 cm⁻¹ indicate the presence of bound and unbound water molecules in the spectrum of **2**. The carbonyl stretching bands the hbn ligands appeared at 1648 cm⁻¹, and 1658 cm⁻¹ respectively for **1** and **2**.

4.2. Structural description of $[\text{Cu}(\text{meoip})(\text{hbn})\cdot\text{H}_2\text{O}]_n$ (**1**)

The asymmetric unit of compound **1** contains a divalent copper atom, a fully deprotonated meoip ligand, an hbn ligand whose central aliphatic chain is disordered over two positions in a 75:25 ratio, and one water molecule of crystallization. A very distorted $\{\text{CuN}_2\text{O}_3\}$ trigonal bipyramidal coordination environment is observed at copper (Fig. 1a), with a τ value of 0.55 [24]. Pyridyl nitrogen donor atoms from two hbn ligands are located in the nominal axial positions of the trigonal bipyramid. Equatorial positions are taken up by single carboxylate oxygen atom donors from

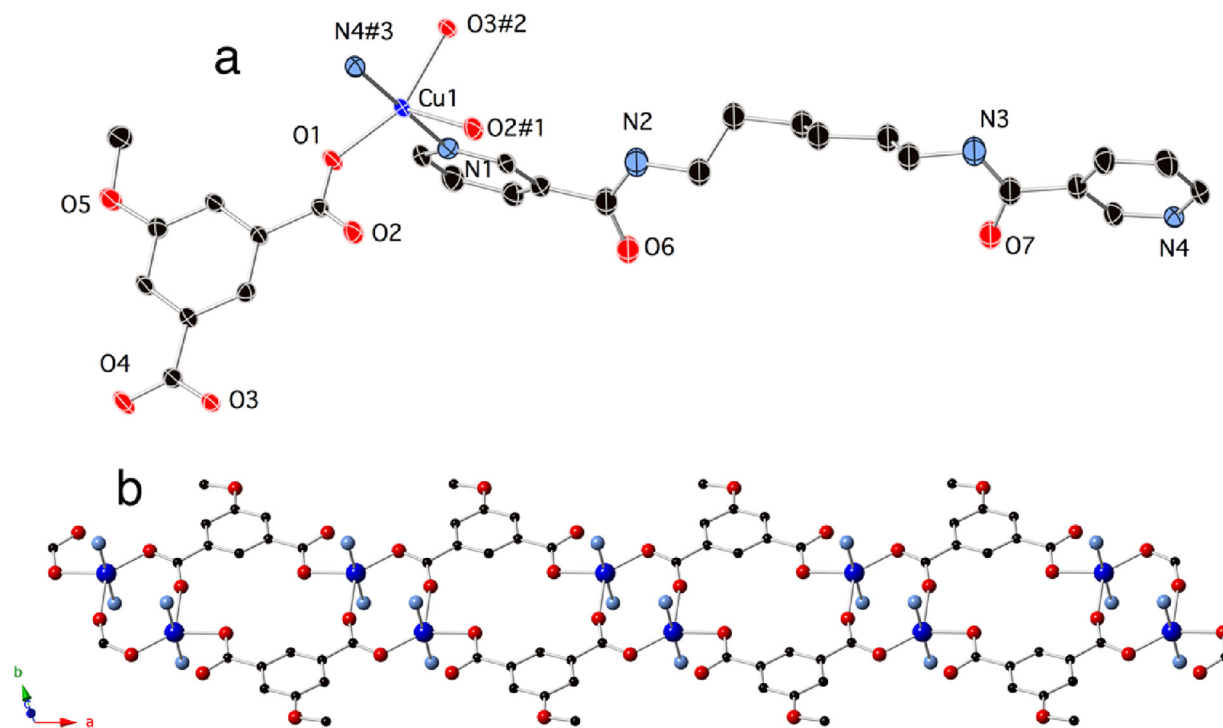


Fig. 1. a) Coordination environment in **1**. Thermal ellipsoids are depicted at 50% probability. Symmetry codes are as in Table 2. b) $[\text{Cu}(\text{meoip})]_n$ chain motif in **1**, showing *syn-skew* bridged $\{\text{Cu}_2(\text{OCO})_2\}$ dinuclear units.

three different meoip ligands. Bond lengths and angles within the coordination sphere are listed in Table 1.

Extridentate meoip ligands with a $\mu_3\text{-}\kappa^3\text{-O:O':O''}$ binding mode connect copper ions into $[\text{Cu}(\text{meoip})]_n$ neutral coordination polymer ribbon motifs (Fig. 1b), with the bridging carboxylate termini constructing $\{\text{Cu}_2(\text{OCO})_2\}$ dimeric units with a $\text{Cu}\cdots\text{Cu}$ internuclear distance of 4.158(2) Å. The full span of the meoip ligands thereby connects the dimeric units to form the $[\text{Cu}(\text{meoip})]_n$ neutral chains, at an interdimer $\text{Cu}\cdots\text{Cu}$ distance of 7.654(4) Å. The $[\text{Cu}(\text{meoip})]_n$ chain motifs are oriented parallel to the *a* crystal direction, and are pillared into $[\text{Cu}(\text{meoip})(\text{hbn})]_n$ coordination polymer layers by the long-spanning hbn ligands (Fig. 2). The dipyrindylamide ligands span an internuclear $\text{Cu}\cdots\text{Cu}$ distance of 18.41(1) Å; the central six-carbon aliphatic chain in the major disorder component has a *gauche-anti-anti* conformation (four-atom torsion angles = 69.4, 175.8, and 172.7°). If the $\{\text{Cu}_2(\text{OCO})_2\}$ dimeric units are considered to be 4-connected nodes, the underlying topology of the $[\text{Cu}(\text{meoip})(\text{hbn})]_n$ layers is that of a (4,4) rectangular grid. Isolated water molecules of crystallization are held within the layer motifs by engaging in hydrogen bonding donation to ligated meoip carboxylate oxygen atoms, and hydrogen bonding acceptance from hbn amide groups (Table 2). Adjacent $[\text{Cu}(\text{meoip})(\text{hbn})]_n$ layers are oriented parallel to the (0 1 1) crystal planes, stacking by means of non-classical C–H \cdots O interactions between hbn pyridyl nitrogen atoms and hbn carbonyl groups in neighboring layers (Fig. S1).

Table 2

Selected bond distance (Å) and angle (°) data for **1**.

Cu1–O1	1.964 (3)	O1–Cu1–N4 ^{#3}	90.56 (12)
Cu1–O2 ^{#1}	2.226 (3)	O3 ^{#2} –Cu1–O2 ^{#1}	89.31 (10)
Cu1–O3 ^{#2}	2.077 (2)	N1–Cu1–O2 ^{#1}	92.34 (12)
Cu1–N1	2.002 (3)	N1–Cu1–O3 ^{#2}	88.24 (11)
Cu1–N4 ^{#3}	2.010 (3)	N1–Cu1–N4 ^{#3}	179.36 (12)
O1–Cu1–O2 ^{#1}	124.48 (10)	N4 ^{#3} –Cu1–O2 ^{#1}	88.29 (12)
O1–Cu1–O3 ^{#2}	146.20 (10)	N4 ^{#3} –Cu1–O3 ^{#2}	91.70 (11)
O1–Cu1–N1	89.13 (12)		

Symmetry transformations: #1 $-x + 2, -y + 1, -z$; #2 $x - 1, y, z$; #3 $x + 1, y + 1, z - 1$.

4.3. Structural description of $\{[\text{Cu}_3(\text{sip})_2(\text{hbn})_3(\text{H}_2\text{O})_4] \cdot 11.5\text{H}_2\text{O}\}_n$ (**2**)

The asymmetric unit of compound **2** consists of a copper atom on a crystallographic inversion center (Cu1), a general position copper atom (Cu2), one trianionic sip ligand, a full hbn ligand (hbn-A), half of another hbn ligand (hbn-B) whose central C–C σ bond is located over another crystallographic inversion center, two aqua ligands, and net five and three-quarters water molecules of crystallization. Two distinct coordination environments are observed in **2** (Fig. 3a). The Cu1 atoms are coordinated in a $\{\text{CuN}_2\text{O}_2\}$ square planar fashion by *trans* carboxylate oxygen atom donors from two sip ligands, and *trans* pyridyl nitrogen atom donors from two hbn-A ligands. In contrast the Cu2 atoms adopt a very distorted $\{\text{CuN}_2\text{O}_3\}$ square pyramidal coordination environment ($\tau = 0.32$). Its basal

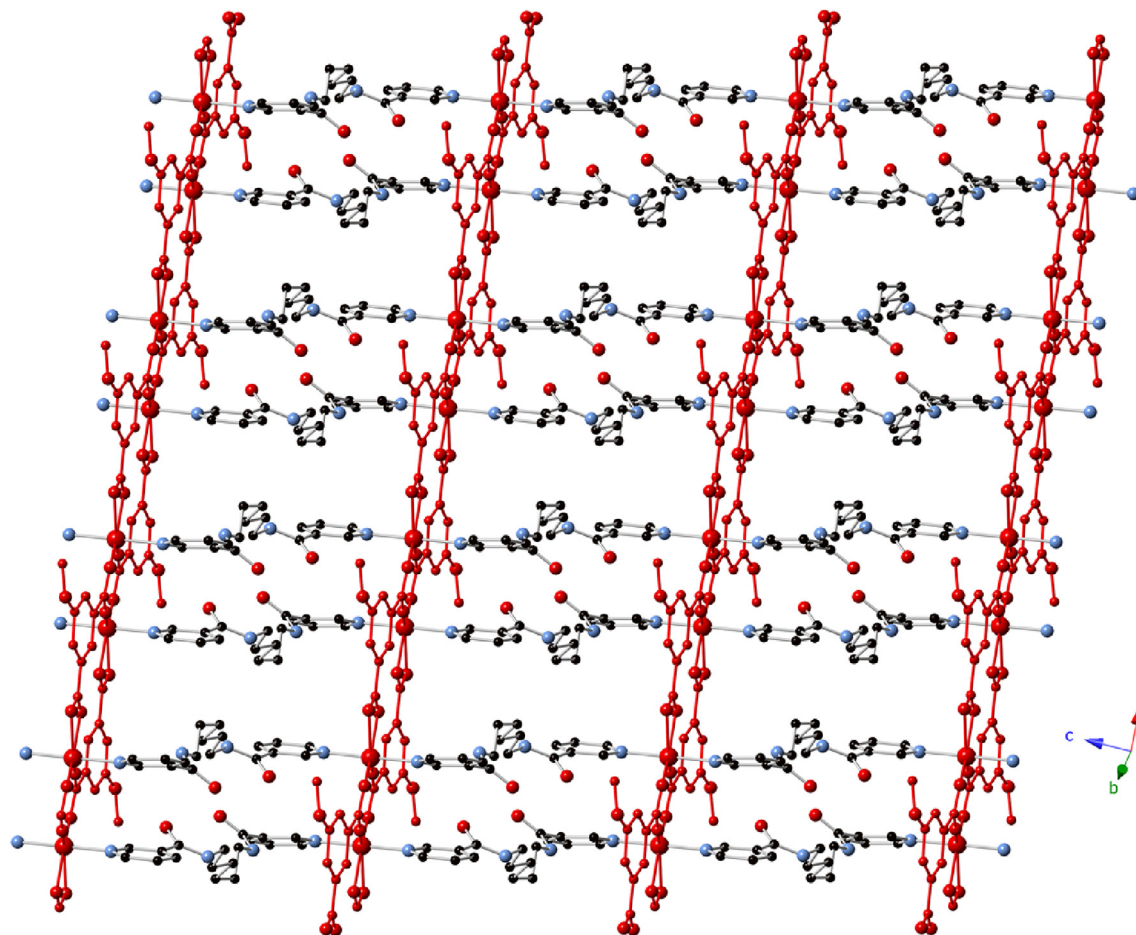


Fig. 2. $[\text{Cu}(\text{meoip})(\text{hbn})]_n$ coordination polymer layer motif in **1**. $[\text{Cu}(\text{meoip})]_n$ chain motifs are drawn in red in the online version of this article. (For interpretation of the references to colour in this figure legend, the reader is referred to the web version of this article.)

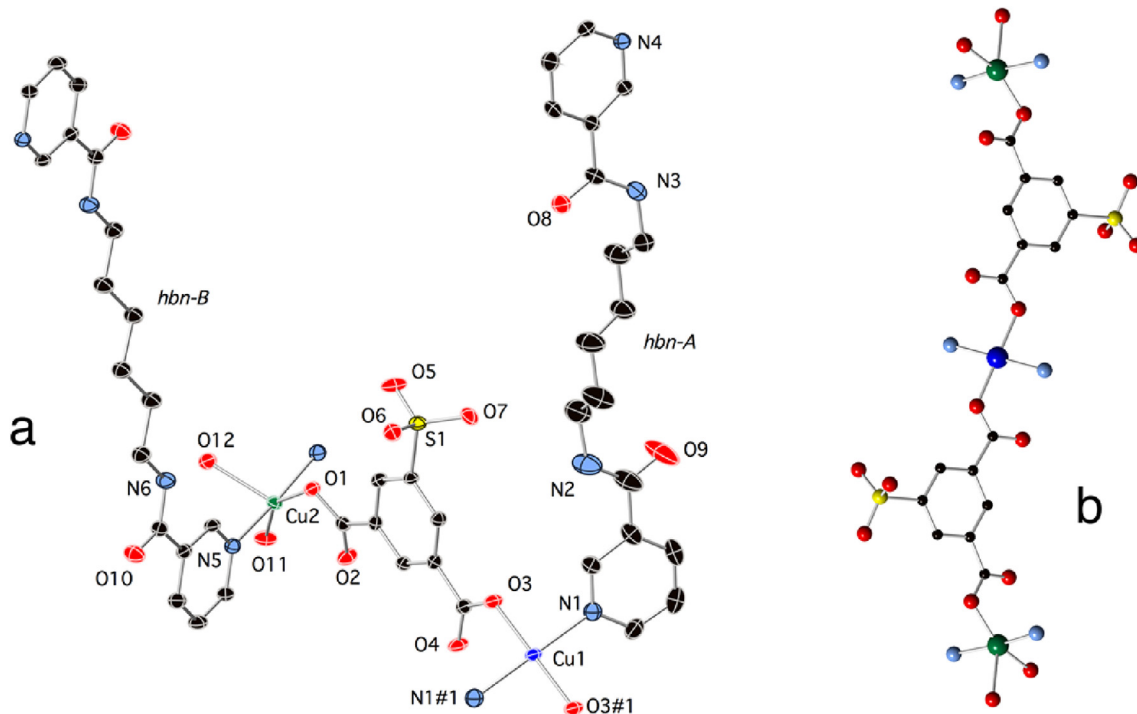


Fig. 3. a) Coordination environments in **2**. Thermal ellipsoids are depicted at 50% probability. Symmetry codes are as in Table 4. b) [Cu₃(sip)₂(H₂O)₄] fragment in **2**.

plane contains *trans* pyridyl nitrogen donor atoms from hbn-A and hbn-B ligands, along with an sip carboxylate oxygen atom and a bound water molecule in *trans* positions. The elongated apical position is filled by another bound water molecule. The sulfonate moiety of the sip ligands does not ligate to copper in **2**. Bond lengths and angles within the disparate coordination environments are listed in Table 3.

The Cu1 atoms on special positions are connected to two Cu2 atoms by pairs of bis(monodentate) sip ligands to construct neutral [Cu₃(sip)₂(H₂O)₄] coordination fragments with a Cu⋯Cu distance of 10.451(4) Å (Fig. 3b). In turn these are linked into [Cu₃(sip)₂(hbn)₃(H₂O)₄]_n coordination polymer layers (Fig. 4) by *gauche-anti-gauche* conformation hbn-A ligands (four-atom torsion

angles = 76.4, 175.8, 71.7°) that connect Cu1 atoms to Cu2 atoms with a Cu⋯Cu distance of 18.964(8) Å, and by *anti-anti-anti* conformation hbn-B ligands (four-atom torsion angles = 177.8, 180, 177.8°) that connect Cu2 atoms to each other with a Cu⋯Cu distance of 17.547(8) Å. Treating the Cu1 atoms as 4-connected nodes and the Cu2 atoms as 3-connected nodes results in a 3,4-connected layer topology with a Schläfli symbol of (4.6²)₂(4²6²8²) (Fig. 5) as computed by TOPOS [25]; this net can be construed as a (4,4) grid with regular, ordered removal of some pillaring ligands. When viewed from the side, the [Cu₃(sip)₂(hbn)₃(H₂O)₄]_n layers show a sawtooth pattern that permits 2D + 2D → 3D parallel interpenetration (Fig. 6). Multifarious hydrogen bonding pathways involving the water molecules of crystallization assist in stabilizing the

Table 3
Hydrogen Bonding Distance (Å) and Angle (°) data for **1–2**.

D–H ⋯ A	d(H ⋯ A)	∠DHA	d(D ⋯ A)	symmetry transformation for A
1				
O1W–H1WA⋯O3	1.98 (2)	2.849 (4)	170 (4)	–x + 2, –y + 1, –z
O1W–H1WB⋯O3	2.12 (2)	2.953 (4)	167 (4)	x–1, y–1, z
N2–H2⋯O1W	2.08 (2)	2.941 (5)	174 (4)	
N3–H3⋯O6	2.11 (2)	2.918 (9)	166 (5)	x–1, y–1, z
N3–H3⋯O6A	2.08 (3)	2.91 (2)	174 (5)	x–1, y–1, z
2				
O5W–H5WA⋯O3W	1.88	2.742 (4)	173.6	–x, –y + 1, –z + 2
O5W–H5WB⋯O6	1.97	2.812 (3)	162.0	x–1, y–1, z
O1W–H1WA⋯O8	1.93	2.745 (3)	155.0	–x–1, –y + 1, –z + 3
O1W–H1WB⋯O4	1.89	2.714 (3)	158.2	
O2W–H2WA⋯O5W	1.89	2.753 (4)	173.7	–x–1, –y + 1, –z + 3
O2W–H2WB⋯O1W	1.89	2.744 (3)	165.8	
O3W–H3WA⋯O2W	2.04	2.866 (5)	158.7	–x, –y + 1, –z + 2
O3W–H3WB⋯O4W	2.07	2.886 (5)	156.7	
O4W–H4WA⋯O9	1.85	2.688 (4)	159.8	x, y, z–1
O4W–H4WB⋯O4	1.88	2.741 (3)	172.7	–x, –y + 1, –z + 2
O11–H11B⋯O2	1.87	2.698 (3)	155.4	–x, –y + 1, –z + 2
O12–H12B⋯O10	1.98	2.815 (3)	158.8	–x + 1, –y + 1, –z + 2
N2–H2⋯O2W	2.06	2.867 (4)	152.6	
N3–H3⋯O6	2.07	2.930 (4)	165.2	–x, –y + 1, –z + 3

Table 4
Selected bond distance (Å) and angle (°) data for **2**.

Cu1–O3	1.964 (2)	O3 ^{#1} –Cu1–N1	88.63 (10)
Cu1–O3 ^{#1}	1.964 (2)	O3 ^{#1} –Cu1–N1 ^{#1}	91.37 (9)
Cu1–N1	2.013 (3)	N1 ^{#1} –Cu1–N1	180.0
Cu1–N1 ^{#1}	2.013 (3)	O1–Cu2–O11	151.40 (9)
Cu2–O1	1.984 (2)	O1–Cu2–O12	121.21 (8)
Cu2–O11	2.024 (2)	O1–Cu2–N4 ^{#2}	85.81 (9)
Cu2–O12	2.207 (2)	O1–Cu2–N5	86.59 (9)
Cu2–N4 ^{#2}	1.999 (2)	O11–Cu2–O12	87.31 (9)
Cu2–N5	1.996 (2)	N4 ^{#2} –Cu2–O11	91.24 (10)
O3–Cu1–O3 ^{#1}	180.0	N4 ^{#2} –Cu2–O12	92.51 (9)
O3–Cu1–N1	91.37 (9)	N5–Cu2–O11	97.84 (9)
O3–Cu1–N1 ^{#1}	88.63 (10)	N5–Cu2–O12	87.11 (9)
		N5–Cu2–N4 ^{#2}	170.88 (10)

Symmetry transformations: #1 $-x, -y + 2, -z + 3$; #2 $x + 1, y + 1, z$.

interpenetrated crystal structure (Table 2). The water molecules form “infinite” tapes with TR(6)A(2)C(2) classification [26] built from flat six-membered circuits with two “para” associated water molecules, linked by short two-molecule chains (Fig. 7). The water tape aggregations are situated in incipient channels parallel to the *b* crystal direction, comprising 16.2% of the unit cell volume according to PLATON [27].

The topology of compound **2** contrasts with a previously reported copper sulfoisophthalate coordination polymer containing the hbn ligand [28]. This phase has a formula of $\{[\text{Cu}_4(\text{sip})_2(\text{OH})_2(\text{H}_2\text{O})_2] \cdot 4\text{H}_2\text{O}\}_n$, with tetranuclear $\{\text{Cu}_4(\mu_3\text{-OH})_2(\text{H}_2\text{O})_2(\text{O}_2\text{C})_4\}$ clusters connected into a binodal (4,8)-connected $(4^4_6^2)(4^{14}_6^{10}8^4)$ topology. In this previously reported

coordination polymer, the hbn ligands bind to six copper atoms, two via their terminal pyridyl ligands, and two at each carbonyl oxygen atom. In compound **2**, the hbn ligands serve only as dipodal tethers.

4.4. Thermal properties

Compound **1** underwent dehydration and partial decarboxylation between 20 and 250 °C, with a mass loss of 5.3% higher than that expected for elimination of one molar equivalent of water (3.3% calc'd). Ligand combustion occurred above 250 °C, with a final mass remnant of 21.7% at 600 °C corresponding roughly to a deposition of CuCO_3 (20.5% calc'd). Compound **2** underwent elimination of its co-crystallized water molecules between 25 and 75 °C, with an observed mass loss of 9.7% corresponding roughly to the expected 10.7% value for loss of 11.5 molar equivalents of water. Its bound water molecules were eliminated between 75 and 140 °C, with a mass loss of 3.3% matching well with the expected value of 3.7% for four molar equivalents of water. Ligand combustion again occurred above 250 °C. The final mass remnant of 25.0% at 600 °C is higher than that expected for deposition of CuCO_3 (19.2% calc'd) indicating the likely presence of uncombusted organic char. The TGA traces for **1** and **2** are shown in Figs. S2–S3, respectively.

5. Conclusions

Divalent copper coordination polymers containing the long-spanning dipyridylamide ligand hbn show a marked structural difference upon altering the 5-position substituent of the anionic

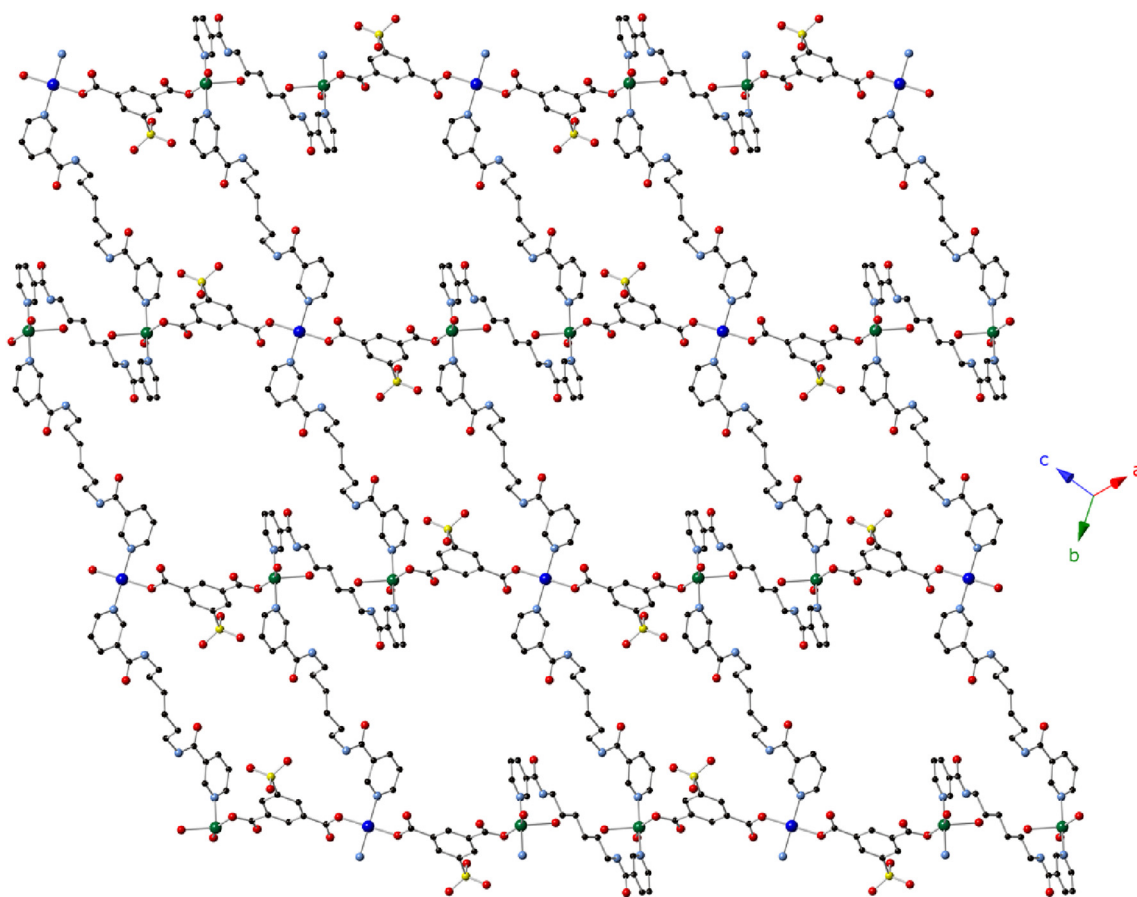


Fig. 4. $[\text{Cu}_3(\text{sip})_2(\text{hbn})_3(\text{H}_2\text{O})_4]_n$ coordination polymer layer motif in **2**.

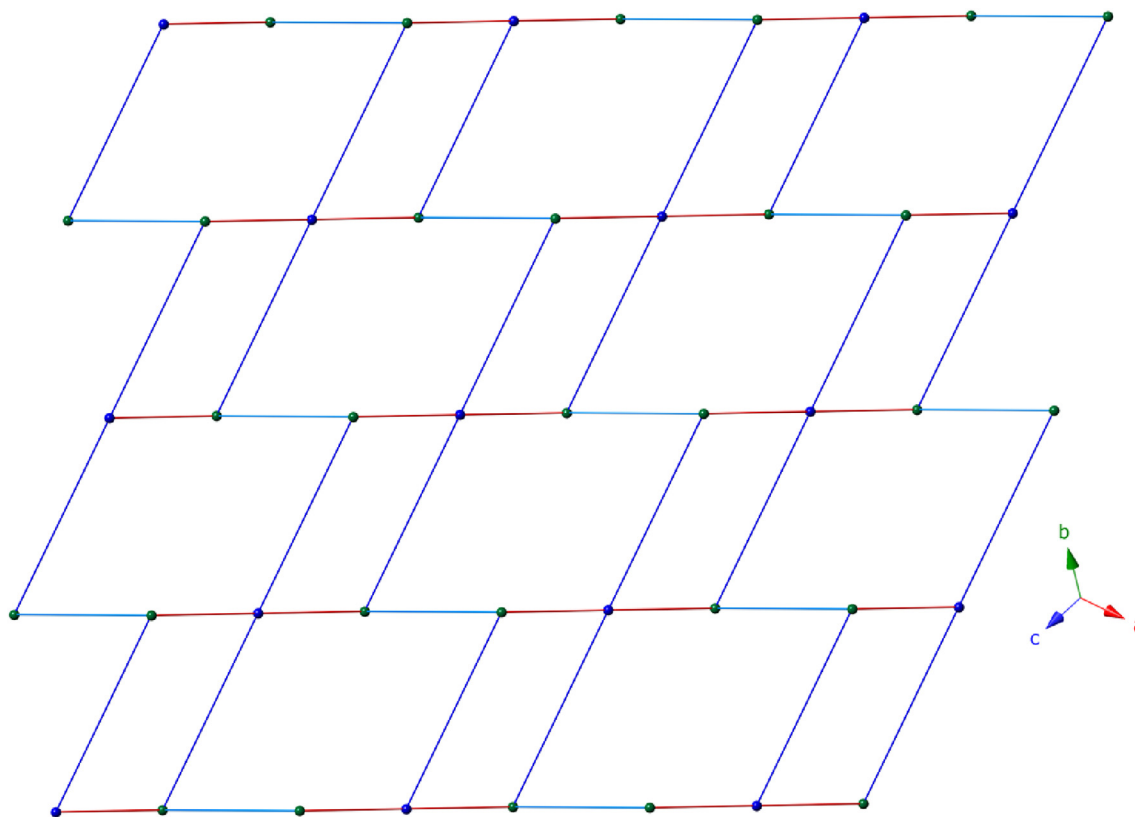


Fig. 5. Schematic representation of the 3,4-connected $\{4.6^2\}_2(4^2 6^2 8^2)$ topology layer in **2**.

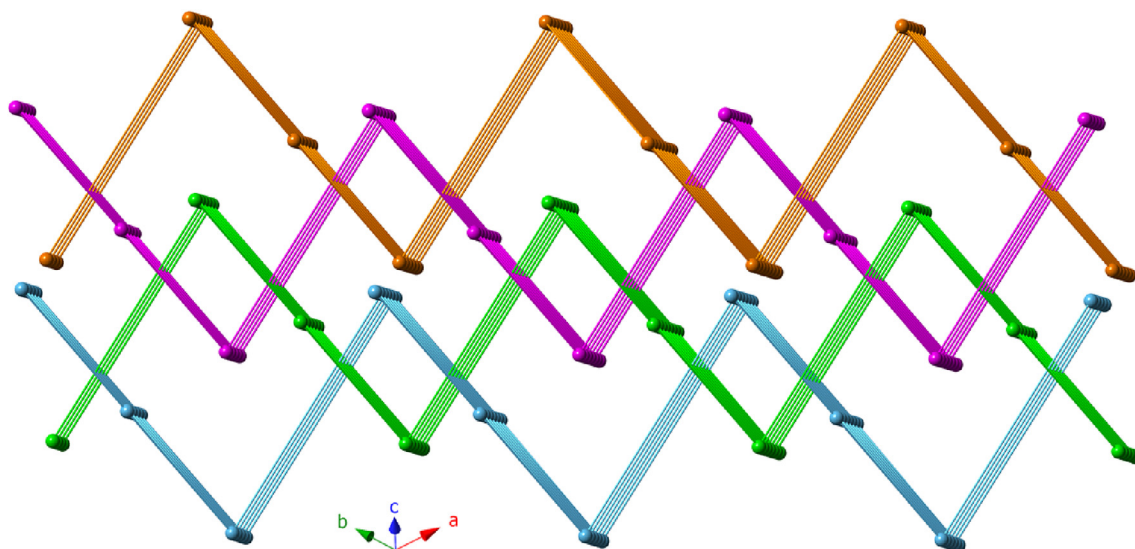


Fig. 6. 2D + 2D \rightarrow 3D parallel interpenetration of sawtooth layer motifs in **2**.

dicarboxylate ligand. A previously reported 5-aminoisophthalate (amip) derivative [16] shows binding of the amino group to copper, resulting in the amip ligand serving as a 3-connected node in a layer structure with a 3,4-connected binodal $(4^2 6^3 8)(4^2 6)$ topology. The 5-position methoxy groups in the meoip ligands in compound **1** in this study are unable to bind to copper, resulting in a $\{\text{Cu}_2(\text{OCO})_2\}$ dinuclear dimer-based decorated (4,4) grid topology. The anionic 5-sulfonate group in the sip ligands in compound **2** in this study also do not bind to copper, but alter the metal to ligand

ratio necessary for a neutral coordination polymer. While compound **2** displays a 3,4-connected binodal net with 4-, 6-, and 8-membered circuits as seen in the amip derivative, it possesses a different $(4.6^2)_2(4^2 6^2 8^2)$ topology. Compound **2** differs markedly in topology from a previously reported related phase that possessed tetranuclear cluster units. The sawtooth undulations in the layer motifs in the sip derivative **2** promote uncommonly encountered 2D + 2D \rightarrow 3D parallel interpenetration and the encapsulation of an intriguing water tape morphology. The topologies of both **1** and

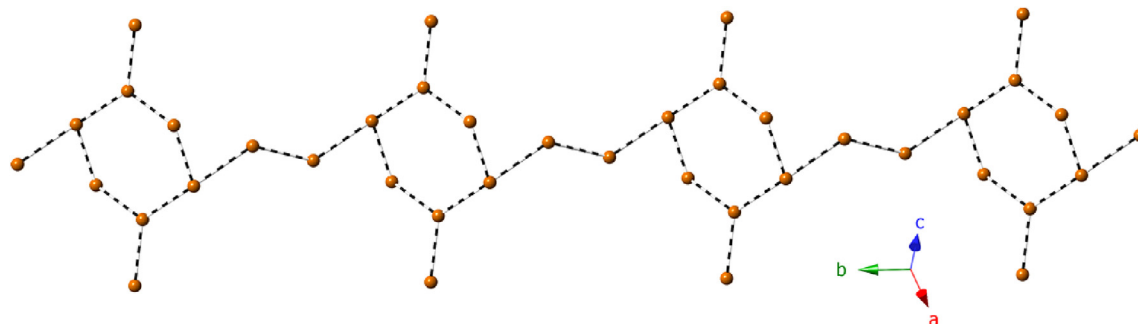


Fig. 7. Co-crystallized water molecule tape in **2**, showing decorated six-membered circuits linked by short two-molecule chains.

2 differ dramatically from the previously reported parent copper isophthalate phase, which manifests a 2D layer structure with a (3,5)-connected $(4^2_6)(4^2_67_8)$ topology [28]. Incorporation of different 5-position substituents on isophthalate ligands continues to diversity the structural topologies possible in divalent metal dual ligand coordination polymers.

Acknowledgements

Support for this work was provided by the Honors College of Michigan State University.

Appendix A. Supplementary data

Supplementary data related to this article can be found at <http://dx.doi.org/10.1016/j.molstruc.2017.01.049>.

References

- [1] L.D. Tran, J.I. Feldblyum, A.G. Wong-Foy, A.J. Matzger, *Langmuir* 31 (2015) 2211.
- [2] M. Foo, R. Matsuda, Y. Hijikata, R. Krishna, H. Sato, S. Horike, A. Hori, J. Duan, Y. Sato, Y. Kubota, M. Takata, S. Kitagawa, *J. Am. Chem. Soc.* 138 (2016) 3022.
- [3] P.F. Gao, L.L. Zheng, L.J. Liang, X.X. Yang, Y.F. Li, C.Z. Huang, *J. Mater. Chem. B* 1 (2013) 3202.
- [4] F. Wang, F. Li, M. Xu, H. Yu, J. Zhang, H. Xia, *J. Lang, J. Mater. Chem. A* 3 (2015) 5908.
- [5] L. Carlucci, G. Ciani, D.M. Proserpio, *Coord. Chem. Rev.* 246 (2003) 247 (and references therein).
- [6] T. Fukushima, S. Horike, H. Kobayashi, M. Tsujimoto, S. Isoda, M. Foo, Y. Kubota, M. Takata, S. Kitagawa, *J. Am. Chem. Soc.* 134 (2012) 13341.
- [7] J. Tao, X.M. Chen, R.B. Huang, L.S. Zheng, *J. Solid State Chem.* 170 (2003) 130.
- [8] a) M. Eddaoudi, J. Kim, N. Rosi, D. Vodak, J. Wachter, M. O’Keeffe, O.M. Yaghi, *Science* 295 (2002) 469;
b) X.-N. Cheng, W.-X. Zhang, Y.-Y. Lin, Y.-Z. Zheng, X.-M. Chen, *Adv. Mater.* 19 (2007) 1494.
- [9] D.J. Tranchemontagne, J.L. Mendoza-Cortés, M. O’Keeffe, O.M. Yaghi, *Chem. Soc. Rev.* 38 (2009) 1257 (and references therein).
- [10] D.S. Zhou, F.K. Wang, S.Y. Yang, Z.X. Xie, R.B. Huang, *CrystEngComm* 11 (2009) 2548.
- [11] D.P. Martin, M.A. Braverman, R.L. LaDuca, *Cryst. Growth Des.* 7 (2007) 2609.
- [12] A.L. Pochodylo, R.L. LaDuca, *CrystEngComm* 13 (2011) 2249.
- [13] B. Xu, J. Lu, M. Cao, L. Han, R. Cao, *Inorg. Chem. Commun.* 14 (2011) 1237.
- [14] A.D. Sample, M.E. O’Donovan, R.L. LaDuca, *Z. Anorg. Allgem. Chem.* 642 (2016) 785.
- [15] L.F. Ma, L.Y. Wang, M. Du, S.R. Batten, *Inorg. Chem.* 49 (2010) 365.
- [16] X. Wang, J. Luan, H. Lin, Q. Lu, C. Xu, G. Liu, *Dalton Trans.* 42 (2013) 8375.
- [17] X. Wang, J. Luan, H. Lin, G. Liu, M. Le, *Polyhedron* 71 (2014) 111.
- [18] T.S. Gardner, E. Wenis, J.J. Lee, *J. Org. Chem.* 19 (1954) 753.
- [19] SAINT, Software for Data Extraction and Reduction, Version 6.02, Bruker AXS, Inc., Madison, WI, 2002.
- [20] SADABS, Software for Empirical Absorption Correction. Version 2.03, Bruker AXS, Inc., Madison, WI, 2002.
- [21] G.M. Sheldrick, SHELXTL, Program for Crystal Structure Refinement, University of Göttingen, Göttingen, Germany, 1997.
- [22] O.V. Dolomanov, L.J. Bourhis, R.J. Gildea, J.A.K. Howard, H. Puschmann, *J. Appl. Cryst.* 42 (2009) 229.
- [23] M. Kurmoo, C. Estournes, Y. Oka, H. Kumagai, K. Inoue, *Inorg. Chem.* 44 (2005) 217.
- [24] A.W. Addison, T.N. Rao, J. Reedijk, J. van Rijn, G.C. Verschoor, *J. Chem. Soc. Dalton Trans.* (1984) 1349.
- [25] V.A. Blatov, A.P. Shevchenko, D.M. Proserpio, *Cryst. Growth Des.* 14 (2014) 3576. TOPOS software is available for download at: <http://www.topos.ssu.samara.ru>.
- [26] a) L. Infantes, S. Motherwell, *CrystEngComm* 4 (2002) 454;
b) L. Infantes, J. Chisholm, S. Motherwell, *CrystEngComm* 5 (2003) 480.
- [27] A.L. Spek, PLATON, a Multipurpose Crystallographic Tool, Utrecht University, Utrecht, The Netherlands, 1998.
- [28] X.L. Wang, P. Liu, J. Luan, H. Lin, C. Xu, *Z. Naturforsch* 67b (2012) 877.